

Modelling Complex Flows in Porous Media by Means of Upscaling Procedures

ANTONIO FASANO AND ANGIOLO FARINA

ABSTRACT. We review a series of problems arising in the field of flows through porous media and that are highly nontrivial either because of the presence of mass exchange between the fluid and the porous matrix (or other concurrent phenomena of physical or chemical nature), or because of a particularly complex structure of the medium. In all these cases there is a small parameter ε , representing the ratio between the microscopic and the macroscopic space scale. Our attention is focussed on a modelling technique (upscaling) which start from the governing equations written at the pore scale, introduces an expansion in power series of ε of all the relevant quantities and eventually leads to the formulation of the macroscopic governing equations at the various orders in ε by a matching procedure, followed by suitable averaging. Two problems will be analyzed with some detail: soil erosion and the dynamics of water ultrafiltration devices. Moreover other problems will be occasionally discussed and open questions will be proposed.

Keywords: Flow in Porous Media, Free Boundary Problems, Fluid Dynamics.
MS Classification 2010: 76S05, 35R35, 76-02

1. Introduction

A porous medium consists of a solid matrix and of connected pores, allowing a fluid to flow through the system. Flows through porous media are found in an impressively large number of applications: oil industry, soil engineering, water recovery and water treatment, agriculture, flows through biological tissues, drying processes, composite materials manufacturing, food industry, geothermal fields, etc.

When dealing with a porous medium at least two spatial scales arise naturally: the macroscopic scale (there can be more than one, depending on the shape and size of the system considered) and the pore scale. Flows through

porous media have been studied extensively either on the basis of empirical laws (formulated in terms of macroscopic quantities such as volumetric discharge and pressure), or taking advantage of the large difference in the above mentioned spatial scales to start from the study of the flow at the microscopic level, then exploiting the smallness of the ratio between characteristic lengths to formulate approximations at various orders and a suitable averaging process, eventually leading to macroscopic governing equations. A procedure of the latter type is called upscaling because of its approach through different scales, but it is also known as homogenization.

For both macroscopic and multi-scale models the literature is huge, even confining (as we shall do in this paper) to the special case of the isothermal flow of an incompressible Newtonian fluid saturating the medium (i.e. completely filling the pores). A list of classical references can be found in [42].

The standard case is the one of saturated incompressible flows with both the fluid and the porous matrix preserving their physical properties. However, very frequently one has to deal with much more complex situations:

- Non-isothermal flows accompanied by phase change (remarkable example: soil freezing and frost heave [33], [54]) or by the polymerization of the fluid (as in composite materials manufacturing [25]), we may include in this category also flows induced by vaporization (the typical case of frying processes [29], [35]).
- Soil hydrology (penetration of rain water [5], dynamics of the vadose and of the phreatic zone [34], [9]).
- Flows of mixtures of immiscible fluids (typical case displacing oil by pushing water in reservoirs [24], [40], [39], [16]).
- Unsaturated flows: here capillarity plays a crucial role and may produce strong dynamical hysteresis [41], [46]; this class includes drying processes [56].
- Flows accompanied by chemical reactions ([15], [44], [7]), including starch hydrolysis (known as gelatinization) in pasta cooking [36], flows accompanied by polymers hydrolysis are also found.
- Flows through deformable porous media, which may exhibit shock propagation phenomena associated to the medium collapse [17], [18], [19], [20].
- Flows accompanied by the growth of biofilms (either spontaneous or induced as in soil bioremediation processes [8], [4]).
- Flows of non-Newtonian fluids.

- Flows in highly heterogeneous, non-isotropic media.
- Flows in media whose grains are in turn porous (with a finer structure), able to release or absorb chemicals (respective examples are: espresso coffee brewing [37], [32], [30]).
- Flows in media whose grains swell, absorbing the fluid and reducing porosity (diapers [31], [26]).
- Flows through evolving biological tissues (heart perfusion, wound healing, tumours, fibrosis processes,). Litterature is huge (see e.g. [48])

In addition, we recall that what has become known as “the porous media equation” (out of our scopes here) deals with gas expansion in a porous medium and is a parabolic equation degenerating at the gas propagation front. Such an equation, exhibiting peculiar properties like finite speed of propagation, waiting time, etc. has received a lot of attention from the mathematicians for decades [1].

The subject of flows through porous media falls naturally in the larger area of mixture theory [50], which studies the mechanics of multi-component systems on the basis of their constitutive laws and specifying the way the various components mutually interact.

Understandably, there is no book dealing with all these aspects, since the variety of problems is too large and, even leaving aside the difficulties connected with modelling, the mathematical aspects involved cover a large spectrum (the elaboration of numerical codes is particularly important). Besides the classical book [2] we quote a recent book on porous media [52] which addresses the question of stability of the flows and is a very recommendable reading.

As we said, we will just be dealing with incompressible, saturated, isothermal Newtonian flows. Our aim is not to go through the classical literature, but instead to review a research direction pursued in a series of very recent papers, in which two kinds of peculiar difficulties are found:

- a) Flows accompanied by mass exchange between the fluid and the solid matrix.
- b) Flows through porous media taking place through micro-channels bounded by porous membranes, with particular references to filters made of a large number of hollow fibres

This are the kinds of “complex” flows referred to in the title.

Coming back to the empirical laws recalled at the beginning of this introduction, we just mention:

- i) the classical Darcy's law [21]

$$\vec{q} = -\frac{K}{\mu} \nabla (p + \rho g z),$$

where K (measured in m^2) is the medium permeability, μ is the fluid viscosity, p is pressure, ρ is the fluid density, g is the gravity acceleration, and z is the upward directed vertical coordinate.

- ii) Forchheimer's law [38], [22]

$$\vec{q} + \alpha |\vec{q}| \vec{q} = -\frac{K}{\mu} \nabla (p + \rho g z),$$

showing a nonlinearity attributable to the fact that for sufficiently large values of discharge the flow leaves the laminar regime becoming turbulent.

- iii) Brinkman's law [10]

$$\vec{q} = -\frac{K}{\mu} \nabla (p + \rho g z) + \lambda \Delta \vec{q},$$

valid for system with high porosity (in that case the presence of the Laplacian is reminiscent of Navier-Stokes equation).

Here we will stay far from the extreme conditions leading to (ii), (iii), remaining in a flow regime that would be certainly Darcy-like in normal cases. Concerning this particular aspect, one of our main purposes is to show that both the presence of mass exchange and the particular complexity of the medium structure may eventually produce a significant deviation from the simple Darcy's law, and at the same time lead to models presenting remarkable mathematical difficulties.

Concerning the problems of class a), we will refer in a more specific way to erosion processes. The main application discussed for problems in class b) is the one of modules for the ultra-filtration of water, but other interesting applications (dialyzers and irrigation pipes) will be marginally discussed.

A peculiar aspect which may have some importance in the problems of class b) is the possible occurrence of slip at the membranes boundaries. The influence of this peculiar dynamical condition on the macroscopic flow will be examined in relation with various geometrical conditions.

2. Flows accompanied by Mass Exchange between the Fluid and the Solid Matrix

2.1. The General Model with Mass Exchange taking place at an Interface

Typical phenomena in this class of flows (keeping the saturation assumption) are:

- Phase change (melting of the solid matrix or solidification of the fluid).
- Deposition of suspended solid particles.
- Erosion (mechanical or chemical) of the solid matrix.
- Growth (or shrinkage) of a biomass film adhering to the solid matrix and metabolizing a pollutant.

We will not consider phase change, since we are confining to isothermal flows, nor the presence of an evolving biomass. In a first instance we will refer to a general law of displacement of the liquid/solid interface. Later on we will consider erosion as an example. For simplicity we will neglect gravity. Such a simplification is usually admissible in a laboratory experiments, but in soils the usual situation is that flows are gravity driven. Changes are not radical (the main difference is the way of selecting the natural pressure scale). In the paper [26] we have illustrated a general model of flow with mass exchange, assuming that the latter process does not influence the physical properties of the fluid. Under the same hypothesis we have treated erosion processes in more detail [13]. The case in which the eroding fluid is considered as an evolving mixture, progressively enriched by the solid particles from the matrix, has been studied in [27].

Since we want to derive some explicit formula we have to deal with a simplified geometry of the flow domain. To this end we replace the chaotic distribution of the pores within the medium with a periodic structure. Various idealizations of the flow domains have been used: the complement of a periodic distribution of equal spheres, a periodic array of identical tubular domains, a periodic array of identical lamellar domains.

To describe flows with mass exchange we adopt the latter geometry, described with the help of fig. 1. The figure represents one half of a single lamella, symmetric with respect to the plane $y^* = 0$, and cut by a plane $z^* = \text{const}$. None of the quantities entering the model depends on the latter coordinate. The complete lamella is obtained by reflection and the whole system is a periodic repetition of the same scheme. As we shall see, any kind of ideal reorganization of the medium structure eventually generates a mathematical

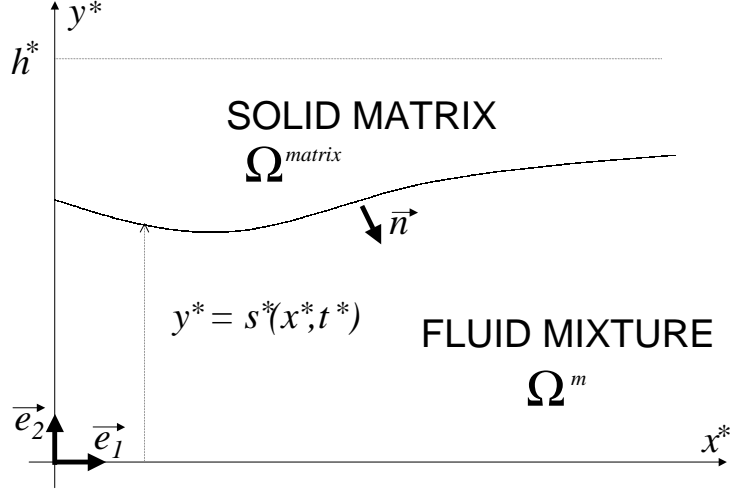


Figure 1: A schematic representation of the system at the pores scale. The fluid is treated as a two-component fluid mixture whose constituents are a fluid and a dispersed solid.

problem exhibiting a dependence of the macroscopic flow on the spatial average of the hydraulic conductivity. We will discuss how to interpret such a nonlocal dependence.

Symbols with a “*” will denote dimensional physical quantities. Likewise ∇^* , Δ^* denote the gradient and the Laplacian with respect to the dimensional space variables. The * will be dropped for the corresponding non-dimensional rescaled variables.

The length of the system in the direction of the main flow (x^*) is L^* . The half-thickness of a lamella is h^* . The small parameter $\varepsilon = h^*/L^*$ is the one providing the double scaling

$$y = y^*/h^*, \quad x = x^*/L^*.$$

ε typically ranges between 10^{-2} and 10^{-4} , or less.

The unknowns of the problem are in general:

- $\vec{v}^{m*} = v_1^{m*}(x^*, y^*, t^*) \vec{e}_1 + v_2^{m*}(x^*, y^*, t^*) \vec{e}_2$, fluid mixture¹ velocity or baricentric velocity (see definition (2)).

¹Quantities related to the mixture will be denoted with the superscript “m”.

- $\vec{v}^{\alpha*}$, $\alpha = s, f$, velocity of the fluid mixture components. In the chosen reference frame the solid matrix is fixed.
- $p^* = p^*(x^*, y^*, t^*)$, fluid mixture pressure.
- $s^* = s^*(x^*, t^*) \geq 0$, channel half-width. In particular, during erosion $\frac{\partial s^*}{\partial t^*} > 0$, i.e. the lumen increases.
- $\vec{u}^* = \vec{u}^*(x^*, t)$, interface velocity.
- $\nu = \nu(x^*, t)$, the variable volume fraction occupied by the solid particles in the mixture and we suppose that during the whole process $0 \leq \nu \leq \nu_o$, with ν_o small enough to consider the mixture a dilute suspension.

The mixture density is (see [50], for instance)

$$\rho^{m*} = \nu \rho^{s*} + (1 - \nu) \rho^{f*}, \quad (1)$$

ρ^{f*} , ρ^{s*} , being the densities of the fluid and solid particles. We thus have

$$\vec{v}^{m*} = \frac{\vec{v}^{s*} \nu \rho^{s*} + \vec{v}^{f*} (1 - \nu) \rho^{f*}}{\rho^{m*}}. \quad (2)$$

We also introduce

$$s = \frac{s^*}{h^*}, \quad \Rightarrow \quad s^* = L^* \varepsilon s, \quad (3)$$

and t_v^* , the characteristic convective time scale

$$t_v^* = \frac{L^*}{v_c^*},$$

with v_c^* characteristic macroscopic fluid mixture velocity, so that

$$t = \frac{t^*}{t_v^*},$$

is the dimensionless time.

Concerning the fluid mixture, we rescale the velocity components in the following way

$$\begin{aligned} v_1^\alpha &= \left(\frac{L^*}{t_v^*} \right)^{-1} v_1^{\alpha*} = \frac{v_1^{\alpha*}}{v_c^*}, \\ v_2^\alpha &= \left(\frac{h^*}{t_v^*} \right)^{-1} v_2^{\alpha*} = \frac{1}{\varepsilon} \left(\frac{L^*}{t_v^*} \right)^{-1} v_2^{\alpha*} = \frac{v_2^{\alpha*}}{\varepsilon v_c^*}, \end{aligned}$$

$\alpha = m, s, f$. Hence

$$\vec{v}^\alpha = \frac{\vec{v}^{\alpha*}}{v_c^*} = v_1^\alpha \vec{e}_1 + \varepsilon v_2^\alpha \vec{e}_2. \quad (4)$$

The natural way of rescaling pressure in our case (for flows which are gravity driven see e.g. [28]) is

$$p = \frac{p^*}{p_c^*}$$

with $p_c^* = \frac{v_c^* \mu^{f*} L^*}{h^{*2}}$, where μ^{f*} is the viscosity of the fluid component.

The interface velocity is rescaled by another characteristic velocity u_c^* , which has to be selected according to the specific process considered. The ratio $t_\Sigma^* = u_c^*/h^*$, defines one more time scale.

For the moment we write the law governing the interface motion in a generic way

$$u^* = \mathcal{G}^*(\cdot), \quad (5)$$

where $u^* = \vec{u}^* \cdot \vec{n}$, (see fig 1.)) is the normal component and \mathcal{G}^* is a function which may depend on a number of variables (s and its derivatives, pressure, tangential stress, etc.).

It is easy to check that passing to non-dimensional variables equation (5) takes the form

$$-\frac{\partial s}{\partial t} = \frac{t_c^*}{t_\Sigma^*} \sqrt{1 + \varepsilon^2 \left(\frac{\partial s}{\partial x} \right)^2} \mathcal{G}(\cdot),$$

in which \mathcal{G} is $\mathcal{O}(1)$, and the initial profile $s(x, 0) = s_o(x)$, is supposed to be such that s'_o , is also $\mathcal{O}(1)$. As a consequence, approximating the square root in the formula above with 1 yields an $\mathcal{O}(\varepsilon^2)$ error.

2.2. Erosion

Summarizing the study performed in [27], the mixture density (1) can be rewritten as

$$\rho^{m*} = \rho^{f*} (1 - \nu(1 - \gamma)),$$

where γ is the ratio $\frac{\rho^{s*}}{\rho^{f*}}$, of the densities of the two pure phases.

In a mechanical erosion process, attributable to the action of the fluid on the interface, the normal velocity of the interface can be defined as

$$u^* = -\kappa^* (|(\mathbf{t}^{m*} \vec{n}) \cdot \vec{t}| - \tau_o^*)_+, \quad (6)$$

where the right hand side is evaluated at the pore wall and:

- \mathbf{t}^{m*} is the fluid mixture Cauchy stress

$$\mathbf{t}^{m*} = -p^* \mathbf{I} + \mu^{m*} \left[\left(\nabla^* \vec{v}^{m*} + (\nabla^* \vec{v}^{m*})^\top \right) - \frac{2}{3} (\nabla^* \cdot \vec{v}^{m*}) \mathbf{I} \right],$$

where μ^{m*} is the fluid mixture viscosity. To be specific, we take

$$\mu^{m*} = \mu^{f*} \psi(\nu), \quad \text{with } 1 \leq \psi(\nu) \leq \psi_M, \quad (7)$$

where, as mentioned, μ^{f*} is the fluid viscosity and ψ is a dimensionless sufficiently regular and bounded function, such that: $\psi(0) = 1$, and $\psi' \geq 0$. For instance, we can use the Einstein's viscosity formula for dilute suspensions, $\psi(\nu) = 1 + \frac{5}{2}\nu$. In such a case $\psi_M = 1 + \nu_o 5/2$.

- κ^* and τ_o^* are given non-negative parameters characterizing the solid material. For simplicity we take them constant, but our analysis can be extended to let them depend on x^* and t^* .
- $(\cdot)_+$ denotes the positive part.

The mass balance of the single species in the mixture is expressed by the system

$$\begin{cases} \frac{\partial \nu}{\partial t^*} + \nabla^* \cdot (\nu \vec{v}^{s*}) = 0, & \text{solid component,} \\ \frac{\partial (1 - \nu)}{\partial t^*} + \nabla^* \cdot ((1 - \nu) \vec{v}^{f*}) = 0, & \text{fluid component.} \end{cases} \quad (8)$$

which, consistently with the saturation condition yields

$$\nabla^* \cdot (\nu \vec{v}^{s*} + (1 - \nu) \vec{v}^{f*}) = 0. \quad (9)$$

representing the so-called saturation constraint for the fluid mixture (see [50], for instance).

If we introduce the solid particle diffusive velocity relative to the mixture, which can be taken of Fickian type

$$\nu \vec{w}^{s*} = -D^* \nabla^* \nu, \quad (10)$$

where D^* is the diffusivity. The saturation condition (9) and the solid mass balance equation (8)₁ we obtain a pair of equations in the unknowns \vec{v}^{m*} and ν

$$\nabla^* \cdot \vec{v}^{m*} = (1 - \gamma) D^* \Delta^* \nu, \quad (11)$$

$$\frac{\partial \nu}{\partial t^*} + \vec{v}^{m*} \cdot \nabla^* \nu = D^* (1 - \nu (1 - \gamma)) \Delta^* \nu, \quad (12)$$

the latter being uniformly parabolic.

The mixture momentum balance is expressed by

$$\rho^{m*} \left[\frac{\partial \vec{v}^{m*}}{\partial t^*} + (\vec{v}^{m*} \cdot \nabla^*) \vec{v}^{m*} \right] = -\nabla^* p^* + \mu^{m*} \cdot \nabla^* \cdot \left\{ \psi(\nu) \left[(\nabla^* \vec{v}^{m*} + (\nabla^* \vec{v}^{m*})^T) - \frac{2}{3} (1 - \gamma) D^* \Delta^* \nu \mathbf{I} \right] \right\}, \quad (13)$$

where the body forces (e.g. gravity) have been neglected, and where (11) has been exploited.

Besides equation (6), describing the erosion process, at the interface we have two more equations for the mass balance of each component in the fluid mixture

$$\begin{aligned} \vec{v}^f \cdot \vec{n} &= \vec{u}^* \cdot \vec{n}, \\ -(1 - \nu) \vec{u}^* \cdot \vec{n} &= \nu \vec{v}^{s*} \cdot \vec{n}. \end{aligned}$$

Next, still on the interface, we prescribe the no-slip condition

$$\vec{v}^{m*} \cdot \vec{t} = 0.$$

On the plane $y^* = 0$, we have the natural symmetry conditions that, written in a dimensionless form, are

$$\begin{aligned} \frac{\partial v_1^f}{\partial y} \Big|_{y=0} &= 0, \\ v_2^f \Big|_{y=0} &= 0, \\ \frac{\partial \nu}{\partial y} \Big|_{y=0} &= 0. \end{aligned}$$

At both ends of the channel, i.e. $x = 0$ and $x = 1$, we specify the pressure

$$p(0, y, t) = p_{in}(t) = \frac{p_{in}^*(t)}{p_c^*}, \quad p(1, y, t) = p_{out}(t) = \frac{p_{out}^*(t)}{p_c^*}.$$

Finally, for what ν is concerned, we set

$$\nu|_{x=0} = 0, \quad (14)$$

i.e. “pure” fluid is entering the channel. At the outflow cross section we put

$$\frac{\partial \nu}{\partial x} \Big|_{x=1} = 0.$$

REMARK 2.1. *We just mention an important analysis concerning the process driving the interface motion, namely energy dissipation. This is necessary to guarantee that such a process satisfies the Clausius-Duhamel inequality (i.e. the second principle of thermodynamics). We omit all the details, because the calculations are quite long (see [26]), and we report the main conclusion.*

Assuming that the Helmholtz free energy ψ^ takes constant values in the solid and in the liquid ψ^{s*} , ψ^{f*} , the required condition is*

$$(\psi^{f*} - \psi^{s*}) \mathcal{G} \geq 0. \tag{15}$$

The physical meaning of this inequality becomes apparent when the interface motion is due to erosion (in that case a glance to fig.1 shows that $\mathcal{G} < 0$). The tangential stress exerted by the flow has the effect of stretching the intermolecular bonds in the solid. Erosion occurs when these bonds are broken, producing the loss of the accumulated potential energy, meaning that $(\psi^{f} - \psi^{s*}) < 0$.*

In the paper [26] we have shown that a macroscopic approach to the same class of problems we are dealing with, based on mixture theory [50], can provide the same results as the upscaling procedure, provided that the constitutive assumptions on partial stresses, interaction forces and Helmholtz free energy are consistent with (15).

2.3. The Upscaling Procedure

Applying the double rescaling procedure to the whole system and introducing the Reynolds and the Péclet number for the microscopic flow

$$\text{Re} = \frac{\rho^{f*} v_c^* h^*}{\mu^{f*}}, \quad \text{Pe} = \frac{D^*}{L^* v_c^*} = \varepsilon \frac{D^*}{h^* v_c^*},$$

we end up with a set of equations containing the parameter ε at various powers. Expanding all relevant quantities in powers of ε , and matching the terms with the same powers in each equation yields the governing system at the various approximation orders. Such a procedure needs the choice of the order of magnitude of Re and of Pe . We select $\text{Re} \leq \mathcal{O}(1)$, meaning that Re is far from ε^{-1} , and $\text{Pe} = \mathcal{O}(\varepsilon)$, though $\text{Pe} = \mathcal{O}(\varepsilon^2)$, would also make sense.

In the series expansion of a function $f(x, y, t)$, the coefficient of the n^{th} , power of ε will be denoted by $f^{(n)}$. After having obtained the differential systems for the desired approximation orders, averaging with respect to the transversal coordinate y across the gap, we end up with the macroscopic equations at the corresponding orders.

For the sake of brevity we omit this rather long calculation and we jump directly to the final 0^{th} , order macroscopic system, referring to [27] for the details.

It turns out that the approximations $p^{(0)}$ and $\nu^{(0)}$, do not depend on y and thus, as well as $s^{(0)}$, they already represent macroscopic quantities. Altogether

they obey the system

$$\begin{cases} \frac{\partial}{\partial x} [s \langle v_1^{(0)} \rangle] = 0, \\ \frac{\partial s}{\partial t} = \left(\left| \frac{\partial p^{(0)}}{\partial x} \right| s - \tau_o \right)_+, \\ \frac{\partial \nu^{(0)}}{\partial t} + \langle v_1^{(0)} \rangle \frac{\partial \nu^{(0)}}{\partial x} = (1 - \nu^{(0)}) \frac{1}{s} \frac{\partial s}{\partial t}, \end{cases} \quad (16)$$

where s stands for $s^{(0)}$ and we have omit the superscript m for the velocity. Here notation has been further simplified setting $\frac{t^*}{t_\Sigma^*} = 1$ and $\text{Pe} = \varepsilon$, which can be obtained by one more rescaling of x , y and t . In the last equation of (16)

$$\langle v_1^{(0)} \rangle = \frac{1}{s} \int_0^s v_1^{(0)}(x, y, t) dy, \quad (17)$$

is the mean longitudinal flow, while the microscopic longitudinal velocity field, obtained through the matching procedure described above, is expressed by

$$v_1^{(0)}(x, y, t) = -\frac{1}{2\psi(\nu^{(0)}(x, t))} \frac{\partial p^{(0)}}{\partial x} (s^2 - y^2). \quad (18)$$

System (2.18) is supplemented with the conditions

$$s(x, 0) = s_o(x), \quad (19)$$

$$p_o(0, t) = p_{in}(t), \quad p(1, t) = p_{in}(t) - \Delta p(t), \quad (20)$$

$$\nu^{(0)}(0, t) = \nu^{(0)}(x, 0) = 0, \quad (21)$$

Note that diffusion has disappeared at this order of approximation.

2.4. Physical Interpretation

Before we discuss the mathematical aspects of the problem (16)-(21), let us ask ourselves what it tells us about Darcy's law, i.e. the way we are used to describe the macroscopic flow.

First of all we must observe that the rescaled variable s has the role of the local porosity and that (17), (18) yield

$$\langle v_1^{(0)} \rangle = -\frac{s^2}{3\psi(\nu^{(0)}(x, t))} \frac{\partial p^{(0)}}{\partial x}. \quad (22)$$

This is the formula we want to interpret in a Darcy-like context. If we multiply this expression by s we obtain the volumetric discharge, which we can now write in the form

$$s \langle v_1^{(0)} \rangle = - \frac{K(s)}{\psi(\nu^{(0)})} \frac{\partial p^{(0)}}{\partial x}, \quad (23)$$

where we have defined the local medium permeability as

$$K(s) = \frac{s^3}{3}. \quad (24)$$

Thus formula (23) agrees with the classical Carman-Kozeny formula [14], but the ratio $\frac{K(s)}{\psi(\nu^{(0)})}$, playing the role of the hydraulic conductivity, is in our case a functional of the pressure gradient. Therefore the parallel with the classical theory is not as strict as it may appear. On the contrary, precisely the nonlocal relationship among the interface, the velocity field and the pressure gradient opens puzzling questions: Why such a feature has never emerged in the literature and what physical meaning should be attributed to it?

With no difficulty we realize that it is not peculiar to the geometry of the lamella. We would have obtained something quite similar adopting e. g. a tubular geometry. The real root of nonlocality is the periodicity constraint, i.e. the assumption that all lamellae (or capillaries) are arranged according to a periodic pattern. This is too much an idealization of the porous medium. Thus a correct use of our results obtained for a single lamella would be to consider a random sequence of initial interface profiles and then averaging the corresponding hydraulic conductivities (24). Such a procedure has been discussed with some detail in [27] on the basis of specific examples.

The main conclusion is that if we take a given initial profile and we consider a sequence of random perturbations depending on a small parameter δ , then at the order $\mathcal{O}(\delta)$, the averaged evolving profile depends on the average of the perturbation. Nevertheless, nonlocality persists at higher orders.

Concerning the evolution of $\nu^{(0)}$, in the last of equations (16), the factor appearing in the source term has the meaning of specific erosion rate, whose effectiveness in increasing $\nu^{(0)}$ is weighted by the available liquid volume fraction. The structure of such equation obviously guarantees that $\nu^{(0)}$ stays below 1.

2.5. Existence and Uniqueness

We recall that the data of the problem are the initial profile $s_o(x)$, the inlet pressure $p_{in}(t)$ and the driving pressure difference $\Delta p(t)$, as in (20). In [27] we have adopted the slight simplification $p_{in} = const.$, and we have treated just the case $\Delta p > 0$, $\tau_o = 0$ (no threshold for erosion). By a solution of (16)-(21) we mean a triple of continuously differentiable functions satisfying all the

equations and such that $s < 1$ (meaning that nowhere the lamella is entirely destroyed). In practice one imposes some upper bound $\bar{s} > \max s_o(x)$.

The main result is the following.

THEOREM 2.2. *If $s_o(x)$, $\Delta p(t)$ are C^1 functions, respectively in $[0, 1]$, $[0, +\infty)$, with $s_o(x)$ bounded away from 0 and 1, and $0 < \Delta p_m < \Delta p(t) < \Delta p_M$, then problem (16)-(21) has a unique solution up to the time (which can be estimated a priori) at which the upper bound \bar{s} , is possibly reached.*

Proof. First of all we introduce $\xi = 1 - \nu^{(0)}$ replacing $\nu^{(0)}$, and set $\hat{\psi}(\xi) = \psi(1 - \xi)$. Next, we eliminate the unknown $p^{(0)}$. This is possible since the first equation in (16) can be interpreted as

$$s \langle v_1^{(0)} \rangle = \frac{\mathcal{F}(t)}{3},$$

where \mathcal{F} is a function to be determined, whose meaning is revealed by (22)

$$\mathcal{F}(t) = -\frac{s^3}{\hat{\psi}} \frac{\partial p^{(0)}}{\partial x}. \quad (25)$$

If from (25) we derive $\frac{\partial p^{(0)}}{\partial x}$, we can exploit the fact that its integral over $(0, 1)$ is $-\Delta p$ to obtain

$$\mathcal{F}(t) = \frac{\Delta p(t)}{\int_0^1 \frac{s^3(x, t)}{\hat{\psi}(\xi(x, t))} dx}, \quad (26)$$

emphasizing the nonlocal structure of the problem, motivated by the necessity of using the boundary conditions for the pressure. At this point we are left with just two unknowns: s and ξ , satisfying the system

$$\begin{cases} \frac{\partial s}{\partial t} = \frac{\hat{\psi}(\xi)}{s^2} \mathcal{F}(t), \\ \frac{\partial \xi}{\partial t} + \frac{\mathcal{F}(t)}{3s} \frac{\partial \xi}{\partial x} = -\frac{\xi \hat{\psi}(\xi)}{s^3} \mathcal{F}(t). \end{cases}$$

For $t = 0$ and $x = 0$, according to (21), we have $\xi = 1$.

We introduce the curve $\Upsilon : r \in (-\infty, 1) \rightarrow (x, t) \in \mathbb{R}^2$,

$$r \xrightarrow{\Upsilon} (x(r), t(r)), \quad \text{with} \quad \begin{cases} x(r) = r \mathcal{H}(r), \\ t(r) = -r \mathcal{H}(-r), \end{cases}$$

where \mathcal{H} is the Heaviside function. This is the curve bearing the data for ξ . We then take the set \mathcal{A} of the pairs (f, g) of continuous functions, defined in $[0, 1] \times [0, T]$, such that:

1. $f(x, t)$ is non decreasing in time, $s_o(x) \leq f(x, t) \leq \bar{s} < 1$, $\forall x \in [0, 1]$, $f(0, x) = s_o(x)$, and f uniformly Lipschitz continuous with constant \mathcal{L} .
2. $1 - \nu_o \leq g(x, t) \leq 1$, $g|_\Gamma = 1$, and g uniformly Lipschitz continuous.

In such a set we define the mapping $\Lambda : (s, \xi) \rightarrow (\sigma, \eta)$ by solving the system

$$\begin{cases} \frac{\partial \sigma^3}{\partial t} = 3\hat{\psi}(\xi) \mathcal{F}_{(s, \xi)}(t), & \text{with } \mathcal{F}_{(s, \xi)}(t) = \frac{\Delta p(t)}{\int_0^1 \frac{s^3(x, t)}{\hat{\psi}(\xi)} dx}, \\ \sigma(x, 0) = s_o(x), \end{cases} \quad (27)$$

and

$$\begin{cases} \frac{3s}{\mathcal{F}_{(s, \xi)}(t)} \frac{\partial \eta}{\partial t} + \frac{\partial \eta}{\partial x} = -3\eta \frac{\hat{\psi}(\xi)}{s^2}, \\ \eta|_\Gamma = 1. \end{cases} \quad (28)$$

We easily realize that, if $(s, \xi) \in \mathcal{A}$, then

$$\Delta p_m \leq \mathcal{F}_{(s, \xi)}(t) \leq \frac{\psi_M \Delta p_M}{s_{o, m}^3}. \quad (29)$$

From (27) we deduce that

$$\sigma^3(x, t) = s_o^3(x) + 3 \int_0^t \hat{\psi}(\xi(x, t')) \mathcal{F}_{(s, \xi)}(t') dt',$$

and we can use the estimate (29) to possibly reduce T so to have $s_o(x) \leq \sigma(x, t) < \bar{s}$ in $[0, T]$.

Turning our attention to (28), we have to distinguish two classes of characteristics, written in the form $t = \hat{t}(x, r)$:

- **Class \mathfrak{C}_1 .** $0 \leq r \leq 1$.

$$\begin{cases} \frac{d\hat{t}(x, r)}{dx} = \frac{3s(x, \hat{t})}{\mathcal{F}_{(s, \xi)}(\hat{t})}, & r \leq x \leq 1, \\ \hat{t}(r, r) = 0, \end{cases}$$

i.e.

$$\int_0^{\hat{t}(x, r)} \mathcal{F}_{(s, \xi)}(\omega) d\omega = 3 \int_r^x s(x', \hat{t}(x', r)) dx'.$$

- **Class \mathfrak{C}_2 .** $r < 0$.

$$\begin{cases} \frac{d\hat{t}(x, r)}{dx} = \frac{3s(x, \hat{t})}{\mathcal{F}_{(s, \xi)}(\hat{t})}, & 0 \leq x \leq 1, \\ \hat{t}(r, -r) = -r, \end{cases}$$

i.e.

$$\int_{-r}^{\hat{t}(x, r)} \mathcal{F}_{(s, \xi)}(\omega) d\omega = 3 \int_0^x s(x', \hat{t}(x', r)) dx'.$$

A careful analysis reveals that the function \hat{t} is such that $\frac{\partial \hat{t}}{\partial r} < 0$ everywhere in its domain of definition, so that from $t = \hat{t}(x, r)$, we can always find $r = \hat{r}(x, t)$. Moreover, we can establish the following estimates

$$\begin{aligned} \left| \frac{\partial \hat{t}}{\partial r} \right| &\geq \mathfrak{m}, \quad \text{with } \mathfrak{m} = \min \left\{ \frac{3s_{o, m}^4}{\psi_M \Delta p_M}, \frac{\Delta p_m s_{o, m}^3}{\psi_M \Delta p_M} \right\}, \\ \left| \frac{\partial \hat{t}}{\partial r} \right| &\leq \frac{3}{\Delta p_m} \max \left\{ 1, \frac{\psi_M \Delta p_M}{s_{o, m}^3} \right\} e^{\frac{1}{\Delta p_m}}, \end{aligned}$$

which eventually enable us to obtain the desired estimates for σ , ξ , namely

$$\begin{aligned} \frac{|\sigma(P_1) - \sigma(P_2)|}{\|P_1 - P_2\|} &\leq \underbrace{\frac{3\psi_M^2 \Delta p_M}{s_{o, m}^5} + \frac{3 \max |s'_o|}{s_{o, m}^2}}_A + \underbrace{\frac{6\psi_M \Delta p_M}{s_{o, m}^5} \max |\psi'| t \mathcal{L}}_{Bt\mathcal{L}}, \\ \frac{|\eta(P_1) - \eta(P_2)|}{\|P_1 - P_2\|} &\leq \mathcal{Q}\mathcal{M}, \end{aligned}$$

for any pair of distinct points $P_1 \equiv (x_1, t_1)$, and $P_2 \equiv (x_2, t_2)$, where

$$\mathcal{M} = \max \left\{ \left(1 + \left(\frac{3}{\Delta p_m} \right)^2 \frac{1}{\mathfrak{m}} \right)^{1/2}, \frac{1}{\mathfrak{m}} \right\},$$

and

$$\mathcal{Q} = \frac{3\psi_M}{s_{o, m}^2} \left(3 + \left(\frac{\max |\psi'|}{\psi_M} \mathcal{G} + \frac{2}{s_{o, m}^2} \mathcal{L} \right) \mathcal{Z} \right),$$

with $\mathcal{Z} = \max \left| \frac{\partial \hat{t}}{\partial r} \right|$. From such estimates it is now clear how to choose the parameters defining the set \mathcal{A} so that:

- (i) Λ maps \mathcal{A} into itself.

(ii) Λ is continuous in the selected norm.

The latter property follows from the inequality

$$\|\sigma_1 - \sigma_2\| + \|\eta_1 - \eta_2\| \leq C(T) \{\|s_1 - s_2\| + \|\xi_1 - \xi_2\|\},$$

which is not difficult to derive. In addition, the function $C(T)$ turns out to be continuous, increasing and vanishing for $T = 0$, thus implying that Λ is a contraction mapping for sufficiently small time intervals. A standard application of Banach and Schauder theorems yields the desired result. \square

REMARK 2.3. *Extending the above Theorem to the case of non-constant inlet pressure and of alternating pressure gradients is not so difficult. On the contrary, eliminating the simplification $\tau_o = 0$ requires much more work, particularly because of the fact that the erosion speed may then exhibit infinitely many isolated zeroes. We left this problem open.*

2.6. Open Problems

By open problems we mean problems still to be studied with the help of the upscaling method. Besides the details mentioned in the previous remarks, a whole category of open problems are the ones with a variable thermal field, possibly accompanied by phase change. The problem of bioremediation is still under investigation, but again we plan to consider the case of an isothermal system with one unique bacterial species and in the presence of a saturated flow, so there is a lot of space for improvement. A glance at the list of processes presented in the introduction suggests many more open problems. In all circumstances a critical analysis should be performed with regard to the geometry of the system. Indeed taking a periodic geometry is important to set up the upscaling procedure, but the passage to a random geometry is eventually necessary. Though we have emphasized the importance of this fact, we believe that this final step deserves further attention.

3. Filtration Through Hollow Fibres

3.1. General Considerations

In many applications a liquid is flowing through very thin hollow membranes, usually packed in large number. For instance this is the case of the ultra-filtration processes used for water depuration. A typical ultra-filtration module houses about 3000 fibres, made of a membrane having a permeability of the order of 10^{-15} m^2 , with pores of $0.1 \text{ }\mu\text{m}$ diameter or less. The hollow fibre²

²Courtesy of Polymem, Toulouse, France.

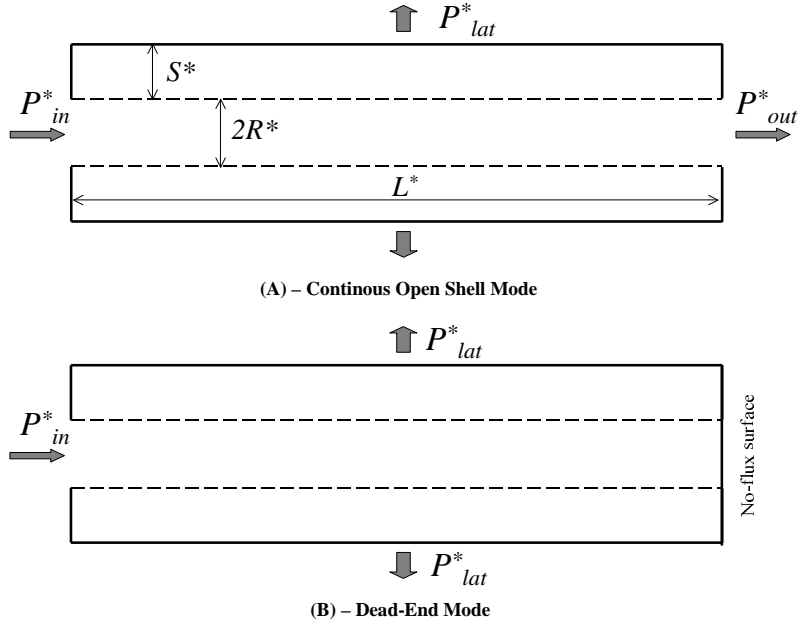


Figure 2: A schematic representation of two flow configurations. (A) Cross flow mode or continuous open shell model. (B) Dead-end mode.

has radii of the order of 0.15 mm and 0.35 mm with a length of 1 m . Such devices can be used in two configurations, illustrated in fig. 2.

Clearly, the dead end mode has a highly effective filtration action, since all the incoming fluid is forced through the membrane. In addition, both configurations can be in-out (as in fig. 2), i.e. with the permeate fluid being collected at the exterior of the fibre, or out-in, with the permeate flowing inside the fibre and the fluid to be filtered injected in the exterior domain.

The open shell mode offers other advantages, connected to the much larger hydraulic conductivity, and it is used in particular when only particles below some size have to be removed. In section 3.2 we will refer specifically to the dead-end, in-out mode.

Arrays of hollow fibres are used in some types of dialyzers, as in fig. 3 (A). The dynamical conditions are now deeply different, since they have substantially different goals.

Dialyzers are designed to perform operations that are close to the ones carried out by the kidneys, [49], [23], [12], [53]. Besides the elimination of chemical substances like urea, a fundamental task of dialyzers is to extract from the

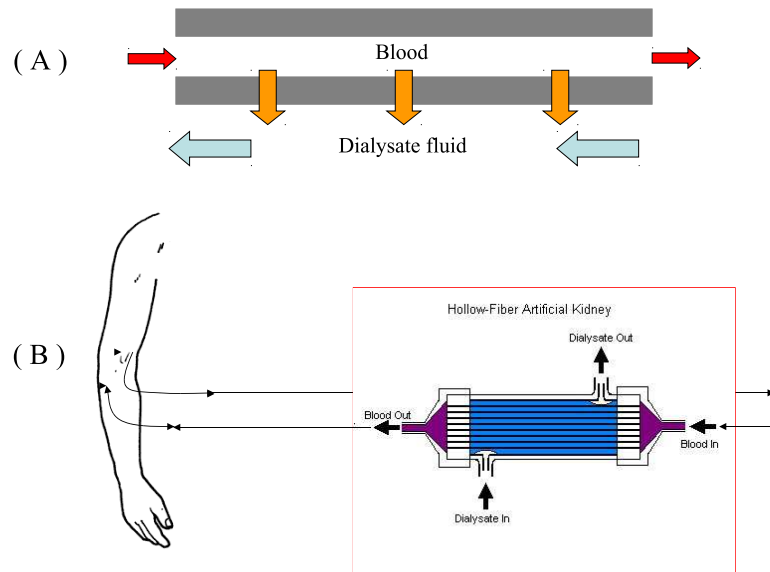


Figure 3: Hemodialysis. (A) The principle of dialysis: blood flows inside and dialysate fluid flows outside of the hollow fiber. The hollow fiber wall acts as a semipermeable membrane. The toxic waste products are removed by either diffusion or by convection. (B) Blood from the patient's artery flows into the device and the treated blood is returned to the patient's vein.

patient's blood plasma about 3 litres of water during the treatment. The target has to be reached in a reasonable time. The duration of the treatment depends on the parameters such the length of the fibres, the pressure gradient driving the blood flow, etc. However conditions that would be favorable from the dynamical point of view (longer fibres, higher values of the discharge) cannot be taken beyond some limit, because the red blood cells are very sensitive to mechanical stresses and can be easily destroyed. Thus it can be said that the actual design of a dialyzer is the sum of numerous and delicate compromises. This explains for instance why the fibres utilized are considerably shorter than the ones mentioned before ($10 \div 20 \text{ cm}$) and thinner (inner radius 0.1 mm , thickness $50 \mu\text{m}$), and the membrane has a permeability in the range $10^{-16} \div 10^{-17} \text{ m}^2$. It is quite obvious that the dead-end configuration is out of question, since it would filter all the blood cells, and only the continuous open shell mode makes sense. Moreover, in order to remove the permeate (now called dialyzate), a counterflow is produced in the exterior of the fibres. Thus, we have two flows

that can be driven independently, controlling two pressure differences (instead of the single transmembrane pressure of the ultrafiltration modules).

Our study on the fluid dynamical behavior of dialyzers is still to be completed and therefore we cannot treat this problem in great detail. We will confine to occasional remarks.

Even farther is the construction of a mathematical model for the kidneys, despite its extreme interest. Indeed kidneys work very much as hollow fibres filters. The hollow fibres are the capillaries. A kidney hosts a large number of units (nephrons), each containing a glomerulus, i.e. a capillary wound up several times and confined in a capsule (Bowman's capsule). The capillary is exposed to a tissue presenting a large number of thin "slots", providing the necessary permeability for filtration. So, while in principle the mechanics is sufficiently clear, the real obstacle is to model the blood flow through the capillary, since none of the existing models for blood rheology can reasonably be applied to capillaries. On the other hand, blood rheology represents a substantial difficulty also in the case of dialyzers (see [45] and the numerous references therein), but the size of the cross section of the fibres in a dialyzer is such that it makes sense to adopt some blood rheology model from the literature, [47] for instance.

One more example, on a totally different scale, is provided by irrigation pipes, which are dead-end tubes laid or suspended on the ground. For small irrigation plants the water filling the pipe under a pressure slightly larger than atmospheric pressure just exudates through the porous pipe wall. The permeability of the material and the geometry of the pipe must be chosen in such a way that water is provided to the ground for the whole pipe length. For large plants the pipes are much longer, are suspended over the ground, and have thick impermeable walls to sustain a larger pressure. A sequence of holes drilled in the walls makes the water drip to the ground. Again, the size and frequency of the holes must be designed to produce an equivalent permeability suitable to obtain the desired performance. Despite the apparent simplicity of the problem, it is by no means trivial.

3.2. Modeling the Single Fibre in the Dead-End Mode

Here we consider an ultrafiltration module of the type described in the previous section, used in the dead-end, in-out configuration (fig. 2). The basic reference is the paper [6]. We just confine to the fluid dynamical problem, neglecting the presence of impurities and the consequent phenomenon of fouling, which consists in the growth of a cake of solid particles over the membrane. In real filtration processes it is necessary to remove the cake periodically (the backwashing process is obtained by inversion of the trans-membrane pressure). Besides fouling, there is also some irreversible blockage of the membrane pores, which eventually reduces its permeability in a drastic way. Thus our study is

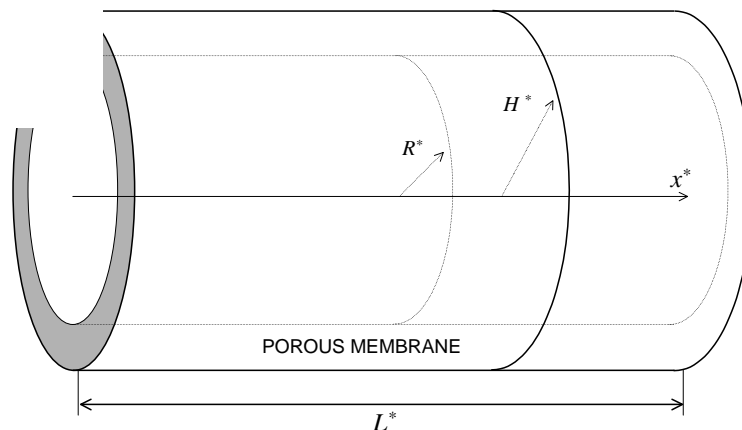


Figure 4: A schematic representation of a single hollow fiber.

just preliminary to a complete investigation of the filtration process. In our analysis we keep an eye on a peculiar aspect that may have some relevance (if not for the ultrafiltration modules, at least for the dialyzers) in all cases in which a fluid flows freely over a porous material: the possible occurrence of a jump of the velocity in the direction tangential to the interface. We want to develop a quantitative theory to understand what is the real influence of this phenomenon. More precisely, we want to suggest a strategy to select the most appropriate level of approximation in modeling the flow through porous pipes. The strategy is based on the values of three parameters:

- The ratio ε between the inner radius R^* and the length L^* of the fibre (or pipe) ($\varepsilon \ll 1$): this is the small parameter which, as in the previous section, allows the use of the double scaling procedure.
- The microscopic Reynolds number Re .
- The non-dimensional parameter B , expressing the magnitude of the slip phenomenon.

Even if our final target is to compute the effective conductivity of a large array of identical fibres, the central element of our study is the model concerning a single fibre, illustrated in fig. 4.

In section 3.4 we shall see how to exploit the model for the single fibre in order to build a scheme for the multi-fibre module.

In the case of filtering fibres the membrane thickness is comparable to the inner radius, i.e.

$$\frac{H^* - R^*}{R^*} = \mathcal{O}(1),$$

while for the exudating irrigation pipes this ratio can be $\mathcal{O}(\varepsilon)$.

In the single fibre flow we have to look for:

- The velocity field in the inner channel

$$\vec{v}^* = v_x^* \vec{e}_x + v_r^* \vec{e}_r.$$

- The velocity field in the membrane

$$\vec{u}^* = u_x^* \vec{e}_x + u_r^* \vec{e}_r.$$

- The pressure field in the inner channel $p_h^* = p_h^*(x^*, r^*, t^*)$.
- The pressure field in the membrane $p_m^* = p_m^*(x^*, r^*, t^*)$.

We rescale x^* by L^* , r^* and H^* by R^* , as usual dropping the “*” to indicate dimensionless variables. Next we introduce a characteristic velocity v_c^* , for the longitudinal flow and a characteristic velocity u_c^* , for the cross flow, such that and we rescale all velocity components as follows

$$v_x^* = \frac{v_x^*}{v_c^*}, \quad v_r^* = \frac{v_r^*}{\varepsilon v_c^*}, \quad u_x^* = \frac{u_x^*}{v_c^*}, \quad \text{and} \quad u_r^* = \frac{u_r^*}{\varepsilon v_c^*}.$$

For the fibres of ultrafiltration modules typical values are $v_c^* \sim 10^{-1}$ m/s, $u_c^* \sim 10^{-5}$ m/s (for dialyzers the respective typical values are $v_c^* \sim 10^{-2}$ m/s, $u_c^* \sim 10^{-4}$ m/s).

The inner channel pressure is rescaled by

$$p_{h,c}^* = \frac{v_c^* \mu^* L^*}{R^{*2}},$$

and the membrane pressure³

$$p_{m,c}^* = \frac{\phi \mu^*}{K^*} R^* u_c^*,$$

where ϕ is the membrane porosity, K^* the membrane permeability and μ^* the liquid viscosity. Note that

$$\Gamma = \frac{p_{m,c}^*}{p_{h,c}^*} = \frac{\phi R^{*4}}{L^{*2} K^*},$$

³Recall that $(H^* - R^*)/R^* = \mathcal{O}(1)$.

for the filtration modules is $\mathcal{O}(1)$, while for dialyzers $\Gamma \sim 10 \div 100$, which rather suggests $\Gamma = \mathcal{O}(1/\varepsilon)$, since for dialyzers $\varepsilon \sim 10^{-2}$. Indeed this parameter should appear in the list of the basic parameters along with ε , Re , \mathbf{B} , but we will develop the theory only for $\Gamma = \mathcal{O}(1)$, to keep the paper in a reasonable size.

Time is rescaled by

$$t_c^* = \frac{L^*}{v_c^*}.$$

Now, for the sake of brevity, we write the governing equations directly in the non-dimensional form. Our plan is, once again, to set up the upscaling procedure.

A) Inner channel.

- Incompressibility

$$\frac{\partial v_x}{\partial x} + \frac{1}{r} \frac{\partial}{\partial r} (r v_r) = 0. \quad (30)$$

- Navier-Stokes

$$\begin{aligned} \frac{\text{Re}}{\varepsilon} \left[\frac{\partial v_x}{\partial t} + v_x \frac{\partial v_x}{\partial x} + v_r \frac{\partial v_x}{\partial r} \right] &= -\frac{1}{\varepsilon^2} \frac{\partial p_h}{\partial x} + \frac{\partial^2 v_x}{\partial x^2} \\ &+ \frac{1}{\varepsilon^2} \frac{1}{r} \frac{\partial}{\partial r} \left(r \frac{\partial v_x}{\partial r} \right), \end{aligned} \quad (31)$$

$$\begin{aligned} \frac{\text{Re}}{\varepsilon} \left[\frac{\partial v_r}{\partial t} + v_x \frac{\partial v_r}{\partial x} + v_r \frac{\partial v_r}{\partial r} \right] &= -\frac{1}{\varepsilon^4} \frac{\partial p_h}{\partial r} + \frac{\partial^2 v_r}{\partial x^2} \\ &+ \frac{1}{\varepsilon^2} \left(\frac{1}{r} \frac{\partial}{\partial r} \left(r \frac{\partial v_r}{\partial r} \right) - \frac{v_r}{r^2} \right), \end{aligned} \quad (32)$$

with the usual definition of the Reynolds number $\text{Re} = \frac{\rho^* v_c^* R^*}{\mu^*}$. We suppose

$$\text{Re} \leq \mathcal{O}(1),$$

that implies laminar flow. In industrial modules Re ranges around 10 (well below $\varepsilon^{-1} \sim 10^4$) while in dialyzers $\text{Re} \sim 1$.

B) Membrane.

- Darcy's law

$$\begin{cases} u_x = -\varepsilon^2 \frac{\partial p_m}{\partial x}, \\ u_r = -\frac{\partial p_m}{\partial r}. \end{cases} \quad (33)$$

- Darcy's law and incompressibility

$$\frac{\partial^2 p_m}{\partial x^2} + \frac{1}{\varepsilon^2} \frac{1}{r} \frac{\partial}{\partial r} \left(r \frac{\partial p_m}{\partial r} \right) = 0. \quad (34)$$

C) Boundary conditions.

- Inlet cross section ($x = 0$, $0 < r < 1$)

$$p_h(0, r, t) = p_{in}(t). \quad (35)$$

- Dead end ($x = 1$, $0 < r < 1$)

$$v_x(1, r, t) = 0. \quad (36)$$

- External membrane surface ($0 < x < 1$, $r = H$)

$$p_m|_{r=H} = \frac{1}{\Gamma} (p_{in}(t) - \Delta p(t)), \quad (37)$$

with $\Delta p > 0$.

- Internal membrane surface ($0 < x < 1$, $r = 1$). Here we have three conditions:

1. Mass conservation

$$v_r(x, 1, t) = -\phi \left. \frac{\partial p_m}{\partial r} \right|_{r=1}. \quad (38)$$

2. Pressure continuity

$$p_h|_{r=1} = \Gamma p_m|_{r=1}. \quad (39)$$

- Beavers–Joseph condition [3], or slip condition

$$-\frac{1}{\mathbf{B}} \left. \frac{\partial v_x}{\partial r} \right|_{r=1} = v_x|_{r=1} + \varepsilon^2 \left. \frac{\partial p_m}{\partial x} \right|_{r=1}, \quad (40)$$

with

$$\mathbf{B} = \frac{\alpha_{\text{BJ}}}{\sqrt{\text{Da}}},$$

where $\text{Da} = \frac{K^*}{R^{*2}}$, and α_{BJ} is the Beavers–Joseph constant (non-dimensional), that can be determined when the microscopic porous structure of the membrane surface is known [43]. Equation (40) shows that

slip is expected to be absent when the coefficient B is large (in our context $B = \mathcal{O}(1/\varepsilon)$), and to be important when $B = \mathcal{O}(1)$. In the form (40) it becomes apparent that Beavers-Joseph condition can be replaced with the Saffman's condition [51]

$$\frac{1}{B} \frac{\partial v_x}{\partial r} \Big|_{r=1} = -v_x \Big|_{r=1}. \quad (41)$$

Some authors, e.g. [55], suggest a way of estimating the parameter in the limit of small Darcy numbers. In our case that theory would lead to the approximate formula

$$B \sim \frac{1}{\sqrt{\phi}} \frac{R^*}{d^*},$$

where d^* is the average diameter of the membrane pores. Applied to the fibres in the ultra-filtration module it gives $B = \mathcal{O}(1/\varepsilon)$, which practically means no slip. The absence of slip is expected in this case, because the dead end condition (36) implies that we are never dealing with large longitudinal velocities. However much smaller values of B are found in many other instances [11].

D) Center line symmetry conditions ($r = 0$).

$$v_r \Big|_{r=0} = 0, \quad \text{and} \quad \frac{\partial v_x}{\partial r} \Big|_{r=0} = 0. \quad (42)$$

REMARK 3.1. Equation (34) for the membrane pressure requires in principle the data for p_m also on $x = 0$, $x = 1$. However, due to the smallness of ε , it is clear that eventually only the radial term of the Laplacian will count. This explain why such conditions do not appear in the system above.

3.3. The Upscaling Procedure for the Single Fibre

As in section 2.3, we expand all dimensionless unknowns as

$$f(x, r, t) = \sum_n f^{(n)}(x, r, t) \varepsilon^n,$$

with the exception of the membrane pressure, for which it is convenient to use the expansion

$$p_m = \frac{1}{\Gamma} \left(p_m^{(0)}(x, r, t) + \varepsilon p_m^{(1)}(x, r, t) + \dots \right).$$

We insert the expansions in the system (30)-(40) (or equivalently (41)) and (42), and we match the terms with equal powers of ε .

At this stage the selection of the order of magnitude of the parameters Re , B , Γ is crucial. We take both Re and Γ to be $\mathcal{O}(1)$, while for B we leave the two possibilities $\text{B} = \mathcal{O}(1)$ (as in the experiments of [3]), and $\text{B} = \mathcal{O}(1/\varepsilon)$ (as in the physical system studied in the previous section).

Omitting intermediate computations, which include some integration and the use of boundary conditions (see [6] for the details), we present the final results.

(A) The zero order approximation. Longitudinal flow in the inner channel

$$v_x^{(0)}(x, r, t) = -\frac{\partial p_h^{(0)}}{\partial x} \left[\frac{1}{2\text{B}} + \frac{1}{4}(1-r^2) \right].$$

Radial flow in the inner channel

$$v_r^{(0)}(x, r, t) = \frac{1}{4} \frac{\partial^2 p_h^{(0)}}{\partial x^2} \left(\frac{r}{\text{B}} + \frac{r}{2} - \frac{r^3}{4} \right).$$

Radial flow in the membrane (the longitudinal velocity is negligible at the zero order)

$$u_r^{(0)} = \frac{[p_{in}(t) - \Delta p(t)] - p_h^{(0)}(x, t)}{\ln H} \frac{1}{r}.$$

For $p_h^{(0)}$, which turns out to be independent of r , we have the equation

$$\frac{\partial^2 p_h^{(0)}}{\partial x^2} = -\frac{4\phi}{\Gamma \left(\frac{1}{\text{B}} + \frac{1}{4} \right)} \frac{\partial p_m^{(0)}}{\partial r} \Big|_{r=1},$$

while, for $p_m^{(0)}$ we find

$$p_m^{(0)}(x, r, t) = p_h^{(0)}(x, t) + \frac{[p_{in}(t) - \Delta p(t)] - p_h^{(0)}(x, t)}{\ln H} \ln r.$$

Thus the whole problem is solved at the zero order if the pressure field is found. Setting

$$\Pi(x, t) = (p_{in}(t) - \Delta p(t)) - p_h^{(0)}(x, t),$$

we formulate the following boundary value problem

$$\begin{cases} \frac{\partial^2 \Pi}{\partial x^2} = C \Pi, & 0 < x < 1, \\ \frac{\partial \Pi}{\partial x} \Big|_{x=1} = 0, \\ \Pi|_{x=0} = -\Delta p(t), \end{cases} \quad (43)$$

where

$$C = \frac{4\phi}{\Gamma\left(\frac{1}{\mathbf{B}} + \frac{1}{4}\right) \ln H} = \frac{256}{\left(\frac{4}{\mathbf{B}} + 1\right)} \frac{K^* L^{*2}}{(2R^*)^4 \ln\left(\frac{H^*}{R^*}\right)}. \quad (44)$$

Problem (43) can be easily solved, getting

$$\Pi = -\frac{\Delta p}{1 + e^{-2\sqrt{C}}} \left(e^{-\sqrt{C}x} + e^{\sqrt{C}(x-2)} \right),$$

and consequently

$$\begin{aligned} p_h^{(0)}(x, t) &= (p_{in}(t) - \Delta p(t)) + \frac{\Delta p(t)}{1 + e^{-2\sqrt{C}}} \left(e^{-\sqrt{C}x} + e^{\sqrt{C}(x-2)} \right), \\ v_x^{(0)}(x, r, t) &= \left[\frac{1}{2\mathbf{B}} + \frac{1}{4}(1 - r^2) \right] \frac{\Delta p(t) \sqrt{C}}{1 + e^{-2\sqrt{C}}} \left(e^{-\sqrt{C}x} - e^{\sqrt{C}(x-2)} \right), \end{aligned}$$

At this point we can compute the zero order approximation of the dimensionless discharge

$$\dot{V}^{(0)} = 2\pi \frac{\phi \Delta p(t)}{\sqrt{C} \ln H} \frac{1 - e^{-2\sqrt{C}}}{1 + e^{-2\sqrt{C}}}, \quad (45)$$

whose corresponding dimensional quantity can be written in the form

$$\dot{V}^{*(0)} = 2\pi \frac{K^* L^{*2}}{\mu^*} \mathcal{K}_{eff} \frac{\Delta p^*}{L^*},$$

exhibiting the dimensionless coefficient \mathcal{K}_{eff} , such that $K^* \mathcal{K}_{eff}$ is the effective permeability of the fibre

$$\mathcal{K}_{eff} = \frac{1}{\sqrt{C} \ln H} \frac{1 - e^{-2\sqrt{C}}}{1 + e^{-2\sqrt{C}}}. \quad (46)$$

Looking at the expression (44) of C , we realize the influence of the various parameters on the coefficient. In particular the influence of slip is quantified. In the limit $\mathbf{B} \gg 1$, (46) agrees with the expression known in the literature [12], with the exception of the factor $(\ln H)^{-1}$, originated from the cylindrical geometry, which however is normally close to 1. Due to such a factor, the effect of slip is progressively diminished if the fibre thickness is increased. It is quite evident that the correction due to slip already at the zero order can be important, since the derivative of \mathcal{K}_{eff} with respect to $1/\mathbf{B}$ in the no-slip limit is $\mathcal{O}(1)$. These considerations are confirmed by the numerical calculations shown in fig. 5 (longitudinal macroscopic velocity profile), and fig. 6 (\mathcal{K}_{eff} vs. H) for various values of \mathbf{B} .

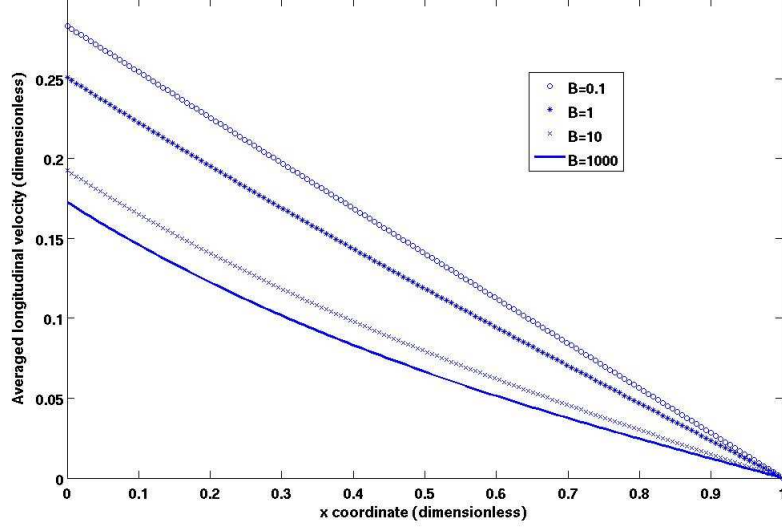


Figure 5: $\langle v_x^{(0)} \rangle$ as a function of x . $\Delta p = 1$, $H = 2$, and $\Gamma = 1$.

(B) The first order correction. We just give the expression of the first order correction of the discharge

$$\begin{aligned} \dot{V}^{(1)} = & \frac{\pi}{6} \left(\frac{1}{B} + \frac{1}{4} \right) \operatorname{Re} M \sqrt{C} \Delta p^2 \left[2 \left(e^{-4\sqrt{C}} - 1 \right) \right. \\ & \left. - \frac{1 + e^{-4\sqrt{C}}}{1 + e^{-2\sqrt{C}}} \left(e^{-2\sqrt{C}} - 1 \right) \right] - \frac{\pi}{4} \operatorname{Re} \frac{C \sqrt{C} \Delta p^2}{\left(1 + e^{-2\sqrt{C}} \right)^2} \\ & \cdot \left(e^{-4\sqrt{C}} - 1 \right) \left(\frac{1}{2B^3} + \frac{1}{2B^2} + \frac{3}{16B} + \frac{1}{48} \right), \end{aligned}$$

where

$$M = \frac{C}{\left(\frac{1}{B} + \frac{1}{4} \right) \left(1 + e^{-2\sqrt{C}} \right)^2} \left[\frac{1}{2B^2} \left(\frac{1}{B} + 1 \right) + \frac{3}{16} \left(\frac{1}{B} + \frac{1}{8} \right) \right].$$

It is interesting to point out that this correction brings a deviation from the Darcy-like behavior, since it introduces a quadratic dependence on the pressure difference Δp , whose importance grows with the Reynolds number. Such an aspect is illustrated in fig.7 (total discharge vs. Δp varying Re from very small to relatively large, $H = 1.5$), and fig. 8 (same, but with $H = 2$).

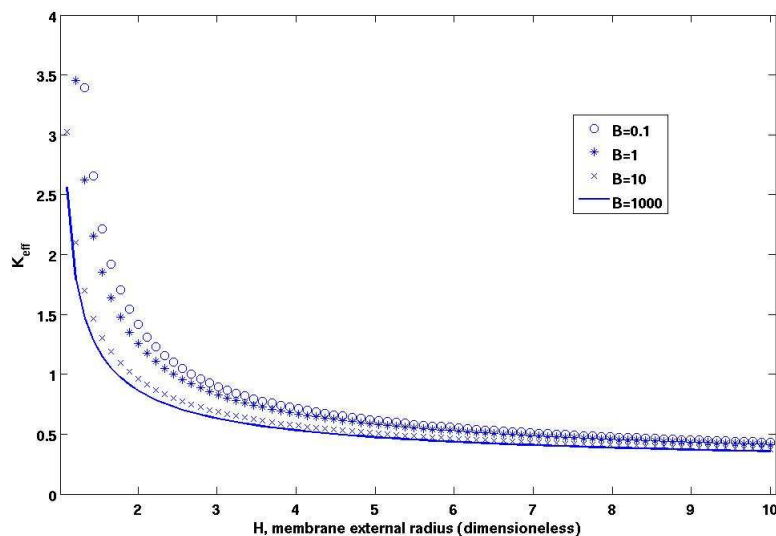


Figure 6: \mathcal{K}_{eff} as a function of H , $1.1 \leq H \leq 10$. $\Gamma = 1$.

3.4. The Fibres Array

The procedure followed for the single fibres can be adapted to describe the multi-fibres system. The idea is that in a periodic array of parallel identical fibres each element is surrounded by a no flux surface, which is a cylinder with an hexagonal cross section. By means of a heuristic argument in [6] we have proved that if R^* , H^* , are comparable and they are also comparable with the distance E^* among the axes of adjacent fibres (which is the practical case), then it is a good approximation to replace the hexagonal cylinder with a circular cylinder. The radius D^* of the latter is taken in such a way to preserve the cross section area of the cylinder. With this criterion $D^* = \sqrt{\frac{\sqrt{3}}{2\pi}} E^*$.

Now, differently from the case of the single fibre, the domain to be considered includes an external corona with $r^* \in (H^*, D^*)$ in which the permeate flows. The surface $r^* = H^*$, becomes an interface quite similar to the interface $r^* = R^*$, where we impose mass balance, pressure continuity, and the Beavers-Joseph (or Saffman) condition, while the boundary $r^* = D^*$, is impervious to the permeate and it is also a symmetry surface for the radial permeate velocity. Thus we have to look for a third velocity field

$$\vec{w} = w_x \vec{e}_x + \varepsilon w_r \vec{e}_r, \quad \text{with} \quad w_x = \frac{w_x^*}{v_c^*}, \quad \text{and} \quad w_r = \frac{w_r^*}{\varepsilon v_c^*},$$

associated to the permeate flux, and to the corresponding pressure field

$$p_v = \frac{p_v^*}{p_{h,c}^*}.$$

The additional differential equations are

$$\frac{\partial w_x}{\partial x} + \frac{1}{r} \frac{\partial}{\partial r} (r w_r) = 0,$$

and

$$\begin{aligned} \frac{\text{Re}}{\varepsilon} \left[\frac{\partial w_x}{\partial t} + w_x \frac{\partial w_x}{\partial x} + w_r \frac{\partial w_x}{\partial r} \right] &= -\frac{1}{\varepsilon^2} \frac{\partial p_v}{\partial x} + \frac{\partial^2 w_x}{\partial x^2} \\ &\quad + \frac{1}{\varepsilon^2} \frac{1}{r} \frac{\partial}{\partial r} \left(r \frac{\partial w_x}{\partial r} \right), \\ \frac{\text{Re}}{\varepsilon} \left[\frac{\partial w_r}{\partial t} + w_x \frac{\partial w_r}{\partial x} + w_r \frac{\partial w_r}{\partial r} \right] &= -\frac{1}{\varepsilon^4} \frac{\partial p_v}{\partial r} + \frac{\partial^2 w_r}{\partial x^2} \\ &\quad + \frac{1}{\varepsilon^2} \left(\frac{1}{r} \frac{\partial}{\partial r} \left(r \frac{\partial w_r}{\partial r} \right) - \frac{w_r}{r^2} \right), \end{aligned}$$

and the additional boundary conditions (which require no further explanation) are

$$p_v|_{x=0} = p_{in}(t) - \Delta p(t),$$

(with Δp playing now the role of the dimensionless transmembrane pressure),

$$\begin{aligned} \frac{\partial w_x}{\partial r} \Big|_{r=D} &= 0, \\ w_r|_{r=D} &= 0, \\ w_x|_{x=1} &= 0, \\ w_r|_{r=H} &= -\phi \frac{\partial p_m}{\partial r} \Big|_{r=H}, \\ \frac{\partial w_x}{\partial r} \Big|_{r=H} &= \text{B} w_x|_{r=H}, \end{aligned}$$

and

$$p_v|_{r=H} = \Gamma p_m|_{r=H}.$$

In [6] the complete theory is illustrated, deriving the zero order approximation of the macroscopic fields. Here we mention just the result concerning the

overall discharge of each fibre in the system (with the exception of peripheral fibres, whose number is however comparatively small, being proportional to the ratio between E^* , and the radius of the entire fibres array)

$$\dot{V}^{(0)} = 2\pi \frac{\phi \Delta p(t)}{\sqrt{A+C} \ln H} \frac{1 - e^{-2\sqrt{A+C}}}{1 + e^{-2\sqrt{A+C}}}, \quad (47)$$

with C is the constant in (44), and

$$A = \frac{16}{H^4} \left\{ \left[4 \left(\frac{D}{H} \right)^4 \ln \left(\frac{D}{H} \right) + 4 \left(\frac{D}{H} \right)^2 - 3 \left(\frac{D}{H} \right)^4 - 1 \right] + \frac{4}{BH} \left(\left(\frac{D}{H} \right)^2 - 1 \right)^2 \right\}^{-1} \frac{K^* L^{*2}}{R^{*4} \ln \left(\frac{H^*}{R^*} \right)},$$

contains the geometrical elements and, once more, the parameter B . Obviously, $A \rightarrow 0$ when $D \rightarrow 0$, and (47) goes back to (45).

3.5. How to select the most suitable Approximation

Though we have studied just the ultrafiltration module, we have collected enough information to suggest a thumb rule to select a reasonable order of approximation when dealing with a flow in a pipe with porous walls.

Table 1 summarizes the choice criterion, referring for simplicity to the case in which the parameter Γ is given and is $\mathcal{O}(1)$.

3.6. Open Problems

As in section 2.6, here too we refer to problems that have to be studied using the procedure of upscaling. The theory just exposed can be generalized in several directions: for instance, we have mentioned that there can be other flow configurations, and in the very same context here examined it would be interesting to see e.g. what happens when the parameter Γ is not $\mathcal{O}(1)$. Of course, the main problem still to be addressed by means of the upscaling technique is the growth of a solid cake over the membrane (fouling) and the irreversible deterioration of the membrane.

Leaving the field of ultrafiltration modules, the most important study to be undertaken, as we have said many times, deals with dialyzers, where the main problem is to tune the various parameters to optimize the treatment, keeping into account the many constraints to be satisfied. Such an investigation is presently in progress.

A less difficult (but still nontrivial) problem is the design of irrigation pipes (in the small and in the large scale). This problem too is being considered within our research group

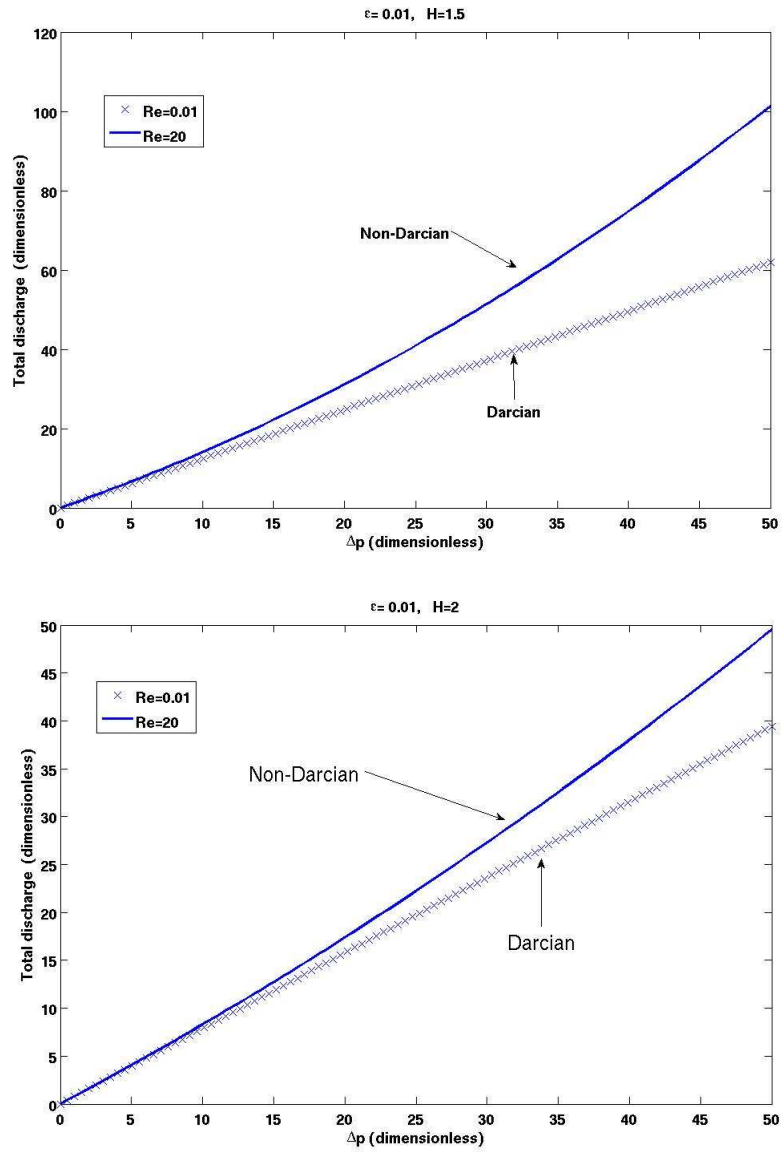


Figure 7: $\dot{V}^{(0)} + \epsilon \dot{V}^{(1)}$, vs. Δp . $B = 1$, $\Gamma = 1$, $H = 1.5$.

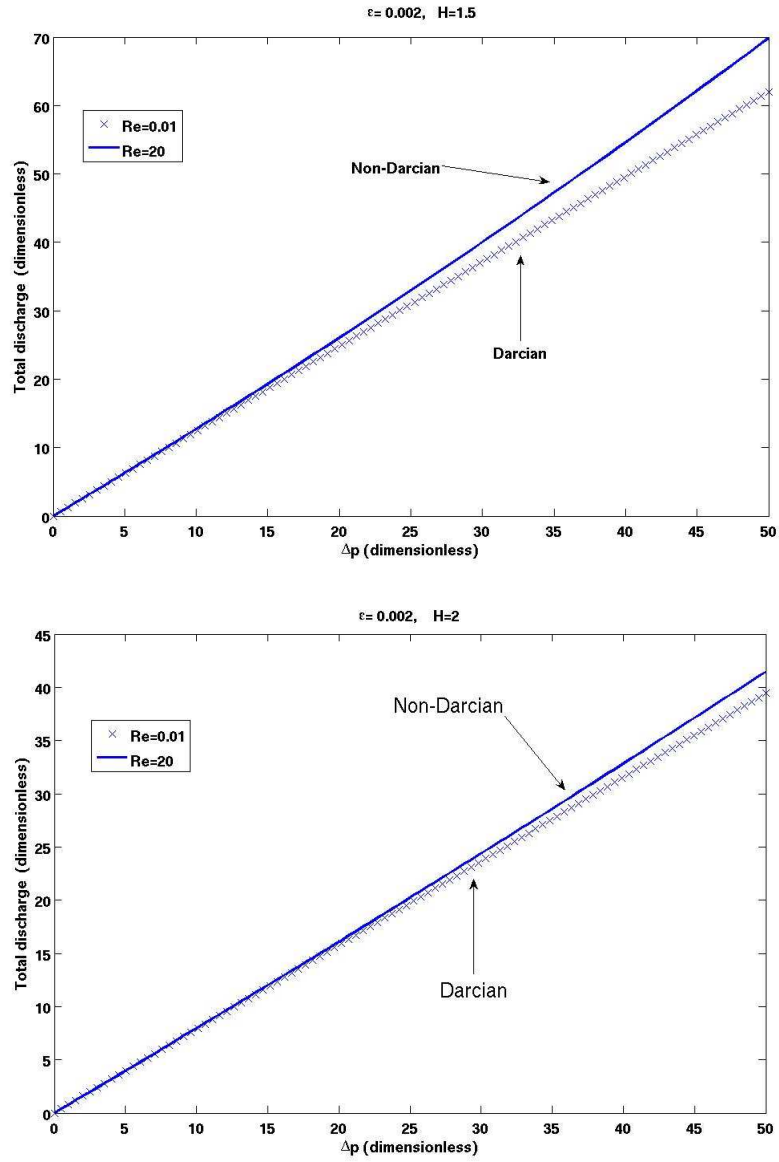


Figure 8: $\dot{V}^{(0)} + \epsilon \dot{V}^{(1)}$, vs. Δp . $B = 1, \Gamma = 1, H = 2$.

Evaluate: ε , B , and Re

• Zero Order

 Theory: $\varepsilon \leq 10^{-3}$
The theory at the ε^0 is accurate enough
Examples:

- Industrial filtration modules.
- Experiments of [1], [8].

- $B = O(1)$. Slip included in the zero-order theory.
(Experiments of [1], [8]).
- $B = O(\varepsilon^{-1})$. Slip is negligible.
(Industrial filtration modules).

• First Order

 Theory: $\varepsilon \approx 10^{-2}$
 $O(\varepsilon)$ corrections are important
Examples:

- Hollow-fiber dialyzers [12].

- $B = O(1)$. Slip included in the zero order **and** first order theory.
- $B = O(\varepsilon^{-1})$. No-slip at the zero order **but** slip at the first order.
(Dialyzers [12]).

- $Re = O(1)$. Non-Darcian flow.
- $Re = O(\varepsilon)$. Darcian flow.

Table 1: Modeling work flow.

References

- [1] D.G. ARONSON, *The porous media equation*, in A. FASANO AND M. PRIMICERIO, *Nonlinear diffusion problems*, Lect. Notes Math. **1124** (1985), 1–46.
- [2] J. BEAR, *Dynamics of fluids in porous media*, American Elsevier (1972).
- [3] G.S. BEAVERS AND D.D. JOSEPH, *Boundary conditions at a naturally permeable wall*, J. Fluid Mech. **30** (1967), 197–207.
- [4] I. BORSI AND A. FASANO, *A general model for bioremediation processes of contaminated soils*, to appear in Int. J. Adv. Eng. Sci. Appl. Math.
- [5] I. BORSI, A. FARINA AND A. FASANO, *On the infiltration of rain water through the soil with runoff of the excess water*, Nonlinear Anal. Real World Appl. **5** (2004), 763–800.
- [6] I. BORSI, A. FARINA AND A. FASANO, *Incompressible laminar flow through hollow fibers: a general study by means of an upscaling approach*, submitted to Z. Angew. Math. Phys.
- [7] I. BORSI, A. FASANO AND L. LENZINI, *Computing the lifetime of granular activated carbon filters by means of travelling waves solutions*, to appear in Appl. Math. Mod.
- [8] I. BORSI, A. FARINA, A. FASANO AND M. PRIMICERIO, *Modelling bioremediation in unsaturated condition and its effect on the soil hydraulic properties*, Appl. Math. **53** (2008), 409–432.
- [9] I. BORSI, A. FARINA AND M. PRIMICERIO, *A rain water infiltration model with unilateral boundary conditions: Qualitative analysis and numerical simulations*, Math. Methods Appl. Sci. **29** (2006), 2047–2077.
- [10] H.C. BRINKMAN, *A calculation of viscous force exerted by a flowing fluid on a dense swarm of particles*, Appl. Sci. Res., **1** (1947), 27–34.
- [11] N.M. BROWN AND F.C. LAI, *Measurement of permeability and slip coefficient of porous tubes*, ASME J. Fluids Eng., **128** (2006), 987–992.
- [12] W.J. BRUINING, *A general description of flows and pressures in hollow fiber membrane modules*, Chem. Eng. Sci., **44** (1989), 1441–1447.
- [13] L. BUCCIANTINI, A. FARINA AND A. FASANO, *On the flow of solid-liquid mixtures with mass exchange*, Netw. Heterog. Media **5** (2010), 69–95.
- [14] P.C. CARMAN, *Fluid flow through a granular bed*, Trans. Instn. Chem. Engrs. **15** (1937), 150–156.
- [15] J. CHADAM, A. PEIRCE AND P. ORTOLEVA, *Stability of reactive flows in porous media: coupled porosity and viscosity changes*, SIAM J. Appl. Math. **51** (1991), 684–692.
- [16] Z. CHEN AND R. EWING, *Mathematical analysis for reservoirs models*, SIAM. J. Math. Anal., **30** (1999), 431–449.
- [17] E. COMPARINI AND M. UGHI, *Shock propagation in a one dimensional flow through deformable porous media*, Meccanica **35**, (2000) 119–132.
- [18] E. COMPARINI AND M. UGHI, *On the existence of shock propagation in a flow through deformable porous media*, Boll. Unione Mat. Ital., **8** (2002), 321–347.
- [19] E. COMPARINI AND M. UGHI, *Shock propagation in a flow through deformable porous media: asymptotic behaviour as the porosity approximates a constant*, Math. Models Methods Appl. Sci. **17** (2007), 1261–1278.

- [20] E. COMPARINI AND M. UGHI, *Shock propagation in a flow through deformable porous media: possible degeneration of the hyperbolic problem*, Adv. Math. Sci. Appl. **17** (2007), 23–35.
- [21] W. DARCY, *Le fontaines publiques de la Ville de Dijon*, Dalmont (1856).
- [22] J. DUPUIT, *Études théoriques et pratiques sur le mouvement des eaux*, Dunod (1863).
- [23] S. ELOOT, D. DE WACHTER, I. VAN TRICH AND P. VERDONCK, *Computational flow in hollow-fiber dialyzers*, J. Artif. Organs, **26** (2002), 590–599.
- [24] M. ESPEDAL AND K.H. KARLSEN, *Numerical solution of reservoir flow models based on large time step operator splitting algorithms*, in M. ESPEDAL, A. FASANO AND A. MIKELIC, *Filtration in porous media and industrial applications*, Lect. Notes Math. **1734** (1998), 9–77.
- [25] A. FARINA AND A. FASANO, *On the analysis of a mathematical model for metal matrix composites manufacturing*, Math. Models Methods Appl. Sci. **13** (2003), 843–874.
- [26] A. FARINA AND A. FASANO, *Incompressible flows through a solid matrix with mass exchange: the multi-scale approach vs. mixture theory*, to appear in Math. Models Methods Appl. Sci.
- [27] A. FARINA AND A. FASANO, *Erosion in porous media caused by the flow of an evolving mixture: an upscaling approach*, to appear in Adv. Math. Sci. Appl.
- [28] A. FARINA AND A. FASANO, *A double scale model for bioremediation processes*, to appear.
- [29] A. FASANO AND A. MANCINI, *A mathematical model for a class of frying processes*, Int. J. Comp. Math. Appl. **53** (2007), 395–412.
- [30] A. FASANO AND A. MIKELIC, *On the filtration through porous media with partially soluble permeable grains*, NoDEA **7** (2000), 141–156.
- [31] A. FASANO AND A. MIKELIC, *The 3-D flow of a liquid through a porous medium with absorbing and swelling granules*, Interfaces Free Bound. **4** (2002), 239–261.
- [32] A. FASANO, A. MIKELIC AND M. PRIMICERIO, *Homogenization of flows through porous media with permeable grains*, Adv. Math. Sci. Appl. **8** (1998), 1–31.
- [33] A. FASANO AND M. PRIMICERIO, *Heat and mass transfer in quasi-steady ground freezing processes*, in M. HAZEWINKEL ET AL., *Proceedings of the first european symposium on mathematics in industry*, Reidel (1986), pag. 31–56.
- [34] A. FASANO AND M. PRIMICERIO, *Liquid flow in partially saturated porous media*, J. I. Maths Appl., **23** (1979), 503–517.
- [35] A. FASANO AND M. PRIMICERIO, *Modelling the onset of vaporization in frying processes with no mechanical deformation*, to appear in J. Food Process Eng..
- [36] A. FASANO, M. PRIMICERIO AND A. TESI, *A mathematical model for spaghetti cooking with free boundaries*, submitted to Netw. Heter. Porous Media.
- [37] A. FASANO AND F. TALAMUCCI, *A comprehensive mathematical model for a multi-species flow through ground coffee*, SIAM J. Math. Anal. **31** (1999), 251–273.
- [38] P. FORCHHEIMER, *Wasserbewegung durch Boden*, Zeits. V. deutsch. Ing. **45** (1901), 1782–1788.
- [39] G. FOTIA AND A. QUARTERONI, *Modeling and simulation of fluid flow in complex porous media*, in the proceedings of the 3rd international congress on industrial

- and applied mathematics (ICIAM95), Akadmie Verlag, Berlin (1996), pag. 55–85.
- [40] D. FUNERO, A. QUARTERONI AND P. ZANOLLI, *An iterative procedure with interface relaxation for domain decomposition methods*, SIAM J. Numer. Anal., **25** (1988), 1213–1236.
- [41] S.M. HASSANIZADEH, M.A. CELIA AND H.K. DAHLE, *Dynamic effect in the capillary pressure–saturation relationship and its impacts on unsaturated flow*, Vadose J. Zone, **1** (2002), 38–57.
- [42] U. HORNUNG, *Homogenization and porous media*, Interdiscipl. Appl. Math. volume 6, Springer, Berlin (1997).
- [43] W. JÄGER AND A. MIKELIĆ, *Modeling effective interface laws for transport phenomena between an unconfined fluid and a porous medium using homogenization*, Transp. Porous Med., **78** (2009), 489–508.
- [44] P. KNABNER AND F. OTTO, *Solute transport in porous media with equilibrium and non-equilibrium multiple site absorption: uniqueness of weak solutions*, Nonlinear Anal. **42** (2000), 381–403.
- [45] M. MASSOUDI AND J.F. ANTAKI, *An anisotropic constitutive equation for the stress tensor of blood based on mixture theory*, Math. Probl. Eng. **2008** (2008) 579172.
- [46] A. MIKELIĆ, *A global existence result for the equations describing unsaturated flow in porous media with dynamic capillary pressure*, J. Diff. Eq. **248** (2010), 1561–1577.
- [47] G. PONTRELLI, *Blood flow through a circular pipe with an impulsive pressure gradient*, Math. Models Methods Appl. Sci. **10** (2000), 187–202.
- [48] A. QUARTERONI, L. FORMAGGIA AND A. VENEZIANI, *Complex systems in biomedicine*, Springer, Berlin (2006).
- [49] N.P. REDDY, *Design of artificial kidneys*, in M. KUTZ, *Biomedical engineering and design handbook, volume 2: applications*, 2nd edition, McGraw Hill, New York (2009).
- [50] K.R. RAJAGOPAL AND L. TAO, *Mechanics of mixtures*, World Scientific, Singapore (1995).
- [51] P. SAFFMAN, *On the boundary condition at a surface of a porous medium*, Stud. Appl. Math. **50** (1971), 93–101.
- [52] B. STRAUGHAM, *Stability and wave motion in porous media*, Springer, Berlin (2008).
- [53] Y. SUZUKI, F. KOHOR AND K. SAKAI, *Computer-aided design of hollow-fiber dialyzers*, J. Artif. Organs, **4** (2001), 326–330.
- [54] F. TALAMUCCI, *Analysis of coupled heat mass transport in freezing porous media*, Surv. Math. Ind. **7** (1997), 93–139.
- [55] F.J. VALDÉS-PARADA, J. ALVAREZ-RAMÍREZ, B. GOYEAU, J.A. OCHOA-TAPIA, *Computation of jump coefficients for momentum transfer between a porous medium and a fluid using a closed generalized transfer equation*, Transp. Porous Med. **78** (2009) 439–457.
- [56] S. WHITAKER, *Simultaneous heat, mass, and momentum transfer in porous media: a theory of drying*, Adv. Heat Transfer, **13** (1977), 119–203.

Authors' addresses:

Antonio Fasano
Dipartimento di Matematica "Ulisse Dini"
Università degli Studi di Firenze
Viale Morgagni 67/A, I-50134 Firenze, Italy
E-mail: fasano@math.unifi.it

Angiolo Farina
Dipartimento di Matematica "Ulisse Dini"
Università degli Studi di Firenze
Viale Morgagni 67/A, I-50134 Firenze, Italy
E-mail: farina@math.unifi.it

Received October 22, 2010

Revised October 28, 2010